Dynamics and Control of a Planar 3-DOF Parallel Manipulator

by
P. A. V. Prasad

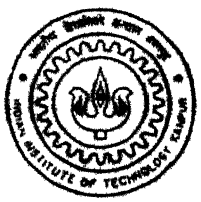

DEPARTMENT OF MECHANICAL ENGINEERING
INDIAN INSTITUTE OF TECHNOLOGY KANPUR

April, 2000

Dynamics and Control of a Planar 3-DOF Parallel Manipulator

A Thesis Submitted
in Partial Fulfillment of the Requirements
for the Degree of
Master of Technology

by

P. A. V. Prasad

to the

Department of Mechanical Engineering
Indian Institute of Technology, Kanpur

April 2000

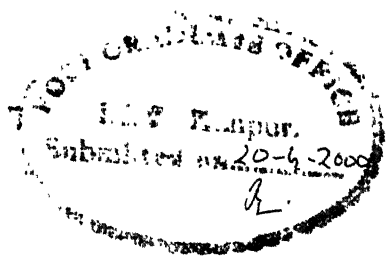

Certificate

This is to certify that the work contained in the thesis entitled "*Dynamics and Control of a Planar 3-DOF Parallel Manipulator*", by *P. A. V. Prasad*, has been carried out under my supervision and that this work has not been submitted elsewhere for a degree.

Bhaskar Dasgupta

Dr. Bhaskar Dasgupta
Department of Mechanical Engg.,
Indian Institute of Technology,
Kanpur.

Acknowledgment

I express my deep sense of gratitude to my thesis advisor Dr. Bhaskar Dasgupta for his excellent guidance, invaluable suggestions, constant support and encouragement during the tenure of this work.

I am very much thankful to Dr. Amitabha Mukherjee for extending the facilities of the Centre for Robotics. His suggestions during thesis proposal has encouraged me in doing the thesis with much vigour.

I am thankful to Mr. Sushmit Sen and Rajender who took a great pain in developing the controller for the manipulator. I am also thankful to Mrs. Anjali Kulkarni and Mrs. Madhuri for their support in clarifying my doubts. I am also thankful to Mr. Jha, Mr. Sharma and Mr. Anil of the manufacturing lab for having helped me in the fabrication of mechanical components.

From my bottom heart i would like to thank my friends boddu, swaroop, shankar, chiller, murthy, kovvi, kakruthi divyesh, sollu pavan, bheem, narasimha, rekula, anaconda sudheer, tanga, GS rao, K sudheer, raju, tulasi, guduru, praveen tayal, madhavayya, gopal and chandrasekhar for their constant help and making my stay at IIT kanpur a pleasant and the most unforgettable part of my life. Special thanks are due to Monica for her constant encouragement when all my friends left. I thank Jogi canteen for providing hot veg rolls and chilled coke when tired.

Finally i thank my parents, brother ravi and all my cousins for their love and affection shown towards me.

Prasad PAV

Abstract

In this thesis, the problem of developing closed-form dynamic equations and designing a PD controller for the 3-DOF planar parallel manipulator is addressed. The overall dynamic model is derived using the Newton-Euler approach. After obtaining the closed-form equations of motion of the manipulator, the PD controller is designed. The purpose of this controller is to maintain the dynamic response of the manipulator in accordance with some prespecified performance criteria. The closed form dynamic equations are non-linear in form and are linearized about a point using first order Taylor's expansion. Hence the linear control laws were applied. State variable analysis is used for determining the dynamic transient response of the system. Position and velocity gains of the system are determined. Simulation results are presented to show the effectiveness of this control approach for both the regulation as well as for tracking the trajectory. The controller developed is implemented on a physical prototype and the experimental results are also reported.

Contents

List of Figures

List of Tables

Chapter 1

Introduction

1.1 Background and Motivation

Parallel manipulators are robotic devices that differ from the traditional serial robotic manipulators by virtue of their kinematic structure. Parallel manipulators are composed of multiple closed kinematic loops. Typically, these kinematic loops are formed by two or more kinematic chains that connect a moving platform to a base, where one joint in each chain is actuated and the other joints are passive. This kinematic structure allows parallel manipulators to be driven by actuators positioned at or near the base of the manipulator.

In contrast, serial manipulators do not have closed kinematic loops and are usually actuated at each joint along the serial linkage. Accordingly, the actuators that are located at each joint along the serial linkage experience additional weight of actuators apart from the link weight, whereas the links of a parallel manipulator generally need not carry the load of the actuators. This allows the parallel manipulator links to be made lighter than the links of a comparable serial manipulator. Hence, parallel manipulators can enjoy the potential benefits associated with light weight construction such as high-speed operation and improved load to weight ratios.

Fig. 1.1 shows the architecture of serial and parallel manipulators. A parallel manipulator consists of two platforms connected by several legs. The top platform is usually free to move and is called the end-effector. The bottom platform is usually fixed and will be called the base. The relative positions of the end-effector and base may be reversed for some applications. The advantage of serial manipulator is large workspace and dextrous maneuverability like human arm, but their load carrying capacity is rather poor due to

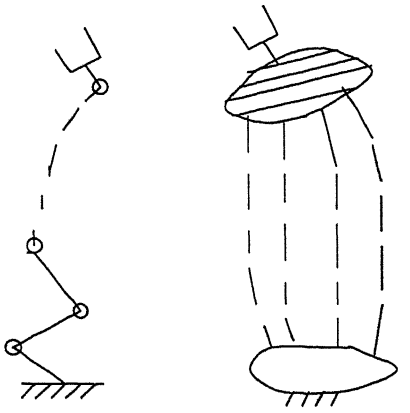

Figure 1.1: Architecture of Serial and Parallel Manipulators

cantilever structure. Because of cantilever beam-like architecture (as we can see in Fig. 1.1), serial manipulators inherently suffer from some drawbacks such as low mechanical stiffness which leads to lower operational accuracy, poor dynamic characteristics and lower load carrying capacity. Therefore, whenever precise positioning and orientation is required, parallel manipulator is a better choice.

Until now, significant work has been done in both the dynamic equations formulation and the control of serial manipulators but not in parallel manipulators. Recently the advantage of parallel manipulators in precise positioning has been understood. In closed loop manipulators, significant work has been done on dynamic equations formulation. Considerable work is done on designing also, but not much work is reported in control of closed-loop manipulators which is a motivation in taking up the work presented in this thesis.

1.2 Manipulator Model and Degrees of Freedom

A 3-DOF planar parallel manipulator is shown in the Fig. 1.2. It has three legs, each leg having two links connected with revolute joints.The end points of the three legs are connected to the platform at A,B,C. All the seven movable links are connected with revolute joints which allow the positioning and the orientation of the platform in a plane. The motors are placed at M1,M2,M3.

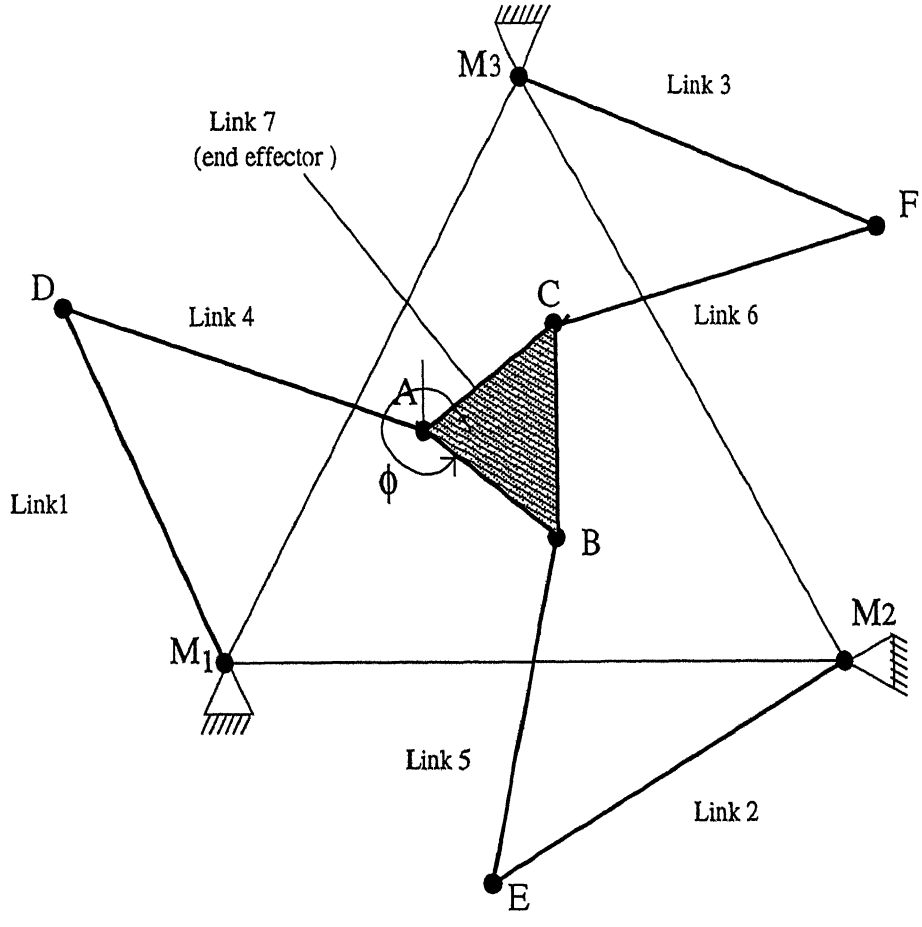

Figure 1.2: Manipulator Model

For a serial manipulator the DOF of the system is given by

$$DOF = \sum_{i=1}^{j} f_i$$

where f_i corresponds to the DOF of the i^{th} joint of the manipulator containing j joints. In general, for serial manipulators, the DOF will be equal to the number of links as each link has a single DOF. For parallel manipulators the formula is (Grubler-Kutzbatch-Chebyshev formula)

$$DOF = n(L - J - 1) + \sum_{i=1}^{j} f_i \tag{1}$$

where L = number of links, J = number of joints, f_i = DOF of i^{th} joint and $n = 6$ for spatial manipulators while $n = 3$ for planar manipulators.

There are total L=8 links (7 movable links and one fixed base), j=9 joints. By using the Eqn. 1 for finding the degrees of freedom, we get that the degrees of freedom for 3-DOF planar parallel manipulator is 3.

1.3 Dynamics

Euler-Lagrange formulation and Newton-Euler formulation are the two broadly adopted approaches for dynamic analysis of robot manipulators. The dynamic equations for the 3-DOF planar parallel manipulator are derived by using Newton-Euler approach because it is computationally efficient for parallel manipulators as shown in Choudhury and Dasgupta[1].

1.4 Servo Control

The inverse problem for manipulator dynamics, namely, the problem of computing the joint torques required to produce given end-effector positions, velocities, and accelerations, has been a computational bottleneck in the control of manipulators. This was

mainly because of the need of computations of torques for trajectories in real time. Because of the importance of the problem and the computational complexity of the equations, the subject has been an attractive area of study in the recent years. This thesis is mainly focussed on the position and tracking of the 3-DOF planar parallel manipulator. Based on inverse dynamic model of the manipulator, PD control scheme is used for controlling the manipulator. Since the equations are non-linear in form, they are linearized about a point using first order Taylor's expansion. Hence the linear control laws were applied. State variable analysis is used for determining the dynamic transient response of the system. The purpose of a positional controller is to servo the motor so that the actual angular displacement of the joint will track a desired path specified by a pre-planned trajectory. The technique is based on using the error signal between the desired and actual angular positions of the joint to actuate an appropriate voltage. In other words, the applied voltage to the motor is linearly proportional to the error between the desired and actual angular displacement of the joint. Position and velocity gains of the system are determined.

1.5 Objective of this Thesis

Developing the dynamic equations, designing a proper proportional-derivative controller and studying the dynamic response behavior of 3-DOF planar parallel manipulator is the aim of the research reported in this thesis. Finally the designed controller is implemented on a physical prototype developed by Kalva [2].

1.6 Literature Review

A general strategy based on the Newton-Euler approach to the dynamic formulation of parallel manipulators is developed by Choudhury and Dasgupta [1]. Marvin Minsky [3] of the MIT was the first person who introduced the term "parallel manipulator" in his early AI memo "Manipulator design vignettes". According to his memo, the parallel concept is best illustrated by the way an animals body is supported by its legs, where several constraints simultaneously determine the relationships of one body to another. The planar 3-DOF manipulator was introduced by Hunt [4] in 1983. Ma and Angeles [5] studied direct kinematics and dynamics of the planar 3-DOF parallel manipulator. In their method,

one of the links of the manipulator is removed virtually so that only one of the three kinematic loops remains, which reduces the non-linear constraint equations from three to one and a technique of 4-bar linkage performance evaluation applied to find the position of end effector. In the dynamics formulation, the natural orthogonal complement is applied, which leads to the algorithm oriented equations of motions involving independent generalized coordinates.

An optimal control approach to robot manipulator pole placement is discussed by Raymond [6]. In their method, Nonlinear control laws are employed to disqualify the nonlinear dynamics of a robot manipulator. The remaining dynamics are controlled by a linear-quadratic (LQ) optimal control scheme which results in the servomechanism problem. The steady-state feedback gains can then be found in closed form as a function of the weighting parameter. A lot of web information on control is collected from the site *www.google.com.*

1.7 Organization of the Thesis

The organization of the thesis is as follows:

Chapter 2 discusses the dynamic equation formulation of the 3-DOF planar parallel manipulator.

Chapter 3 deals with the controller design for controlling the manipulator.

Chapter 4 deals with the Simulation Results and Discussions.

Chapter 5 discusses about control of DC motors, software and hardware implementation required for 3-DOF planar parallel manipulator.

Chapter 6 discusses the Experimental Results obtained from the physical prototype.

Chapter 7 discusses the Concluding remarks and Suggestions for further work.

Chapter 2

Dynamic Formulation of the Manipulator

2.1 Procedure

The Newton-Euler method of dynamic formulation is based on the direct application of Newton's law and Euler's equation in the form

$$\sum \mathbf{F} = m\mathbf{a} \tag{1}$$

and

$$\sum \mathbf{M} + \sum \mathbf{r} \times \mathbf{F} = \mathbf{r}_{cg} \times m\mathbf{a} + \mathbf{I}\boldsymbol{\alpha} + \boldsymbol{\omega} \times \mathbf{I}\boldsymbol{\omega} \tag{2}$$

to individual bodies. This yields three scalar equations (for planar case) for each body. In the present work, the dynamic formulation of parallel manipulators is considered in task-space because of the simplicity of the resulting equations. The salient features and steps of the strategy (see [1]) are described as following:

- For each leg,
  - Find the position, velocity and acceleration of the platform-connection-point from (or in terms of) the task-space coordinates and their derivatives.

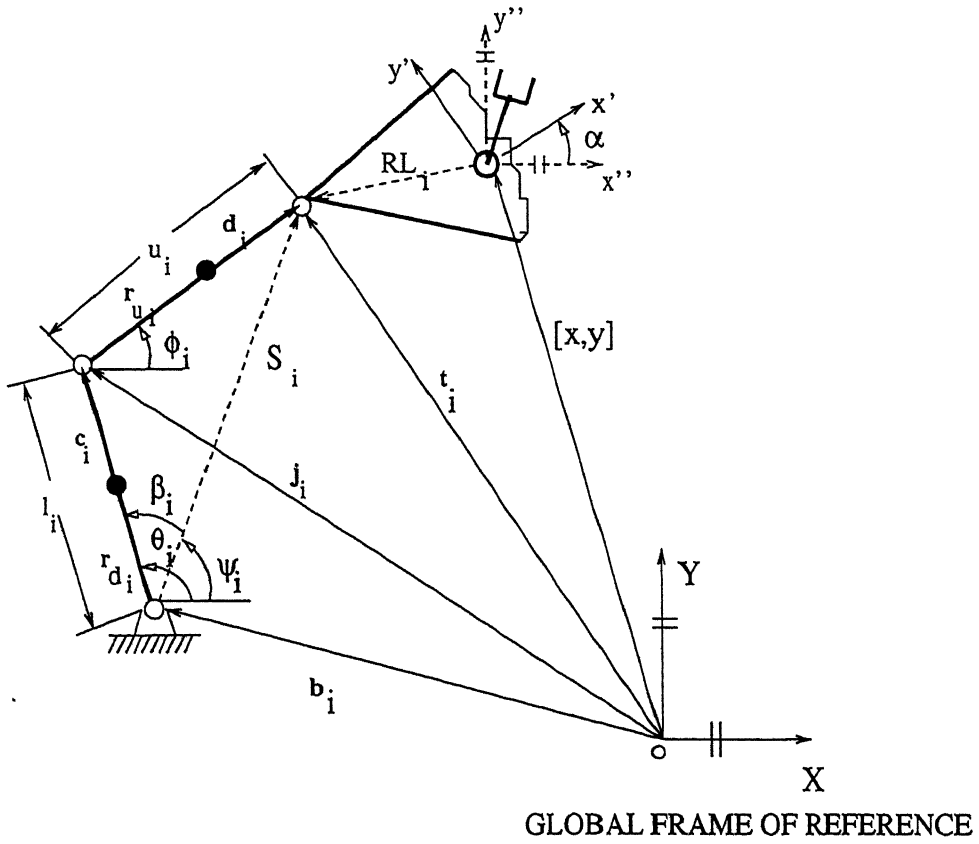

Figure 2.1: Notations of the Leg

- Solve the kinematics of the leg for position, velocity and acceleration.
- Now, first obtain the moment equilibrium equation for the upper link about the intermediate joint. Then obtain moment equilibrium equation for both the links about the base joint.
- From the equations obtained above, solve the reaction at the platform-connection-point in terms of the actuations in the leg and the platform accelerations $\ddot{\mathbf{X}}$

- Consider equilibrium of the platform and write Newton's and Euler's equations for it. Simplify the equations to the standard form (resulting in the closed-form dynamic equations).

2.2 Notations for the Leg

The notations for the leg as shown in Fig.2.1 are

$\mathbf{c}_i$ The unit vector along the lower link of i-th leg

$\mathbf{d}_i$ The unit vector along the upper link of i-th leg

$\mathbf{j}_i$ The joint vector of the intermediate revolute joint

$\mathbf{b}_i$ Base point of the i-th leg

$\mathbf{t}_i$ Platform connection point

$\mathbf{T}$ End-effector point

$\mathbf{S}_i$ Vector joining the base to the platform connection point

α Orientation of the platform

$\mathbf{X}$ Task space position of the end-effector

$\mathbf{R}$ The rotation matrix

x'-y' The frame fixed to the platform

x"-y" The frame on the platform and parallel to the Global Frame of reference

$\mathbf{d}_\perp$ represents the vector $\mathbf{d}$ rotated anti-clockwise by a right angle

2.3 Inverse Kinematics of the Manipulator

With the previous notation for the leg vector and denoting the lengths of the lower and upper links by l and u respectively, the position kinematics of a single leg is determined as follows:

The position,velocity and acceleration of the platform connection points is

$$\mathbf{t}_1 = \begin{bmatrix} x \\ y \end{bmatrix} + \begin{bmatrix} cos(\alpha) & -sin(\alpha) \\ sin(\alpha) & cos(\alpha) \end{bmatrix} \begin{bmatrix} -p/2 \\ -q/3 \end{bmatrix}$$

$$\mathbf{t}_2 = \begin{bmatrix} x \\ y \end{bmatrix} + \begin{bmatrix} cos(\alpha) & -sin(\alpha) \\ sin(\alpha) & cos(\alpha) \end{bmatrix} \begin{bmatrix} p/2 \\ -q/3 \end{bmatrix}$$

$$\mathbf{t}_3 = \begin{bmatrix} x \\ y \end{bmatrix} + \begin{bmatrix} cos(\alpha) & -sin(\alpha) \\ sin(\alpha) & cos(\alpha) \end{bmatrix} \begin{bmatrix} 0 \\ 2q/3 \end{bmatrix}$$

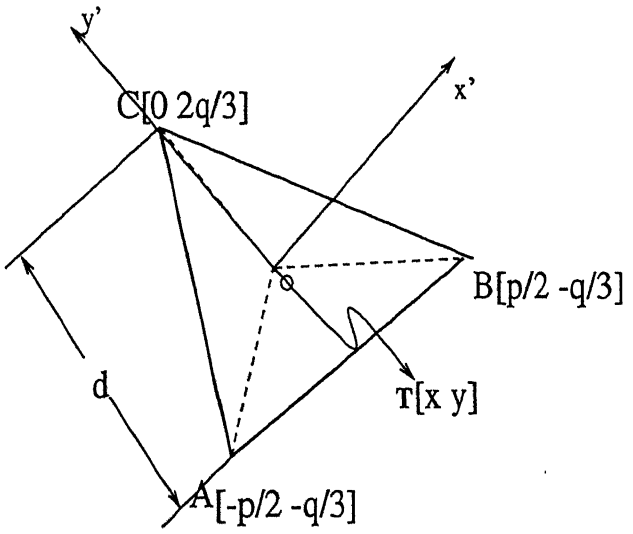

AB='p' is the side of each platform

'q' is the height of the platform

'o' is the end effector position [x y]

Figure 2.2: The positions of platform connection points with respect to platform frame

$$\dot{\mathbf{t}}_1 = \begin{bmatrix} \dot{x} & \dot{y} \end{bmatrix} + \begin{bmatrix} -sin(\alpha) & -cos(\alpha) \\ cos(\alpha) & -sin(\alpha) \end{bmatrix} \begin{bmatrix} -p/2 \\ -q/3 \end{bmatrix} \dot{\alpha}$$

$$\ddot{\mathbf{t}}_1 = \begin{bmatrix} \ddot{x} & \ddot{y} \end{bmatrix} + \begin{bmatrix} -cos(\alpha) & sin(\alpha) \\ -sin(\alpha) & -cos(\alpha) \end{bmatrix} \begin{bmatrix} -p/2 \\ -q/3 \end{bmatrix} \dot{\alpha}^2 + \begin{bmatrix} -sin(\alpha) & -cos(\alpha) \\ cos(\alpha) & -sin(\alpha) \end{bmatrix} \begin{bmatrix} -p/2 \\ -q/3 \end{bmatrix} \ddot{\alpha}$$

For the sake of convenience, the subscripts are omitted from now.
Considering the kinematics and dynamics of one leg.

$$\mathbf{S} = \mathbf{t} - \mathbf{b}\,; \qquad L = \|\mathbf{S}\|; \qquad \mathrm{s} = S/L$$

$$\psi = tan^{-1}(S_y/S_x); \qquad \beta = cos^{-1}(\tfrac{l^2+L^2-U^2}{2lL}); \qquad \theta = \psi \pm \beta$$

unit vectors **c** and **d** along the lower and upper links obtained from

$$\mathbf{c} = \begin{bmatrix} cos(\theta) \\ sin(\theta) \end{bmatrix}; \qquad \mathbf{j} = \mathbf{b} + l\mathbf{c}; \qquad \mathbf{d} = (\mathbf{t} - \mathbf{j})/u \quad \text{and} \quad \psi = tan^{-1}(d_y/d_x)$$

Angular velocities of the lower and upper links are given by

$$\begin{bmatrix} \dot{\theta} \\ \dot{\phi} \end{bmatrix} = \mathbf{A}_1^{-1}\dot{\mathbf{t}}$$

where

$$\mathbf{A}_1 = \begin{bmatrix} -lsin(\theta) & -usin(\phi) \\ lcos(\theta) & ucos(\phi) \end{bmatrix}$$

and the linear velocity of the intermediate joint is

$$\dot{\mathbf{j}} = l\mathbf{c}_\perp\dot{\theta}$$

After carrying out the accelerations analysis, the angular accelerations of the two links are given by

$$\begin{bmatrix} \ddot{\theta} \\ \ddot{\phi} \end{bmatrix} = \mathbf{A}_1^{-1}(\ddot{\mathbf{t}} + \mathbf{V}_0)$$

and the final expressions for the accelerations of the centres of gravity for the respective lower and upper links are given by

$$\mathbf{a}_d = \frac{\mathbf{r}_{d\perp}\mathbf{d}^T}{l\,sin(\phi-\theta)}\ddot{\mathbf{t}} + \mathbf{V}_d$$

where $\mathbf{r}_d$ and $\mathbf{r}_u$ denote the vector from the base point to the cg (centre of gravity) of the lower link and that from the intermediate joint to the cg of the upper links, respectively, and

$$\mathbf{V}_0 = l\dot{\theta}^2\mathbf{c} + u\dot{\phi}^2\mathbf{d}$$

$$\mathbf{V}_d = \frac{\mathbf{r}_{d\perp}\mathbf{d}^T\mathbf{V}_0}{l\,sin(\phi-\theta)} - \mathbf{r}_d\dot{\theta}^2$$

$$\mathbf{V}_u = \frac{\mathbf{c}_\perp\mathbf{d}^T\mathbf{V}_0}{sin(\phi-\theta)} - \dot{\theta}^2 l\mathbf{c} - \mathbf{r}_u\dot{\phi}^2 - \frac{\mathbf{r}_{u\perp}\mathbf{c}^T\mathbf{V}_0}{usin(\phi-\theta)}$$

2.4 Dynamics of the Manipulator

Now, coming to the dynamic analysis of the leg, we first consider the moment equilibrium of the upper link about the point **j** and thereafter we take into account the moment equilibrium of both the links as a whole about base point **b** (Since the manipulator works in the horizontal plane, the gravity effects are zero). This gives rise to two equations, namely

$$u\mathbf{d}_\perp^T\mathbf{F} = -m_u\mathbf{r}_{u\perp}^T\mathbf{a}_u - I_u\ddot{\phi}$$

and

$$\mathbf{S}_\perp^T\mathbf{F} = -m_u(l\mathbf{c}+\mathbf{r}_u)_\perp^T\mathbf{a}_u - m_d\mathbf{r}_{d\perp}^T\mathbf{a}_d - I_d\ddot{\theta} - I_u\ddot{\phi} + \tau$$

where **F** denotes the reaction force exerted by the leg at output point and τ gives the input torque.

These two equations can be solved together for **F** and we get

$$\mathbf{F} = \begin{bmatrix} F_x \\ F_y \end{bmatrix} = \frac{1}{lsin(\phi-\theta)}\tau\mathbf{d} - \mathbf{Q}\ddot{\mathbf{t}} + \mathbf{U} \tag{3}$$

where

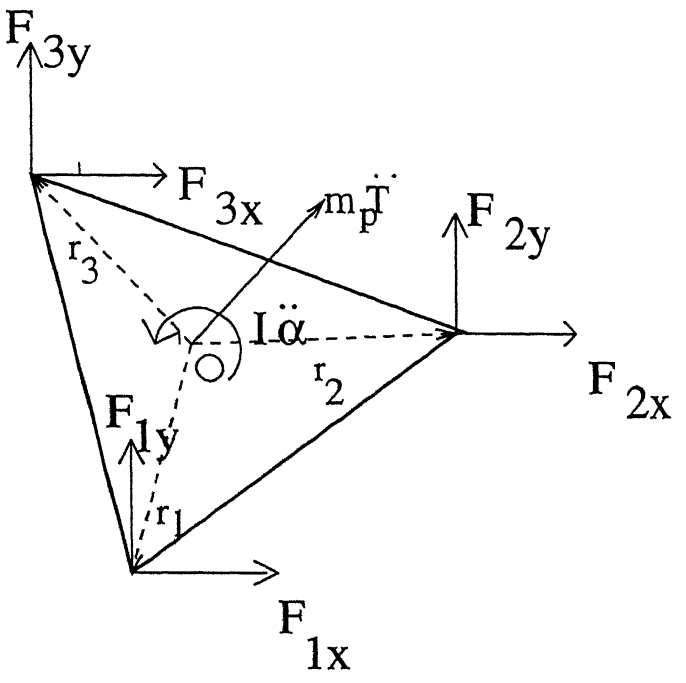

Figure 2.3: Force components on the Platform

$$\mathbf{Q} = \frac{1}{lusin^2(\phi-\theta)}\left[m_u l(\mathbf{d}\mathbf{d}^T u - \mathbf{c}\mathbf{r}_{u\perp}^T)\mathbf{c}_\perp\mathbf{d}^T - \mathbf{d}\mathbf{c}_\perp^T\mathbf{r}_{u\perp}\mathbf{c}^T + \frac{l}{u}(m_u\mathbf{r}_u^2 + I_u)\mathbf{c}\mathbf{c}^T + \frac{u}{l}(m_d\mathbf{r}_d^2 + I_d)\mathbf{d}\mathbf{d}^T\right.$$

$$\mathbf{V} = m_u l(u\mathbf{d}\mathbf{c}_\perp^T)\mathbf{V}_u + m_d u\mathbf{d}\mathbf{r}_{d\perp}^T\mathbf{V}_d - \frac{I_d u}{lsin(\phi-\theta)}\mathbf{d}\mathbf{d}^T\mathbf{V}_0 - \frac{I_u l}{usin(\phi-\theta)}\mathbf{c}\mathbf{c}^T\mathbf{V}_0$$

$$\mathbf{U} = \frac{\mathbf{Gg}-\mathbf{V}}{lusin(\phi-\theta)}$$

$$\mathbf{G} = m_u l(u\mathbf{d}\mathbf{c}_\perp^T) + m_d u\mathbf{d}\mathbf{r}_{d\perp}^T$$

After getting the force components (both x and y) at the platform connection points, the dynamic equations of the platform can be written as

$$F_{1x} + F_{2x} + F_{3x} = m_p\ddot{x}_p$$
$$F_{1y} + F_{2y} + F_{3y} = m_p\ddot{y}_p$$
$$\mathbf{r}_1 \times \mathbf{F}_1 + \mathbf{r}_2 \times \mathbf{F}_2 + \mathbf{r}_3 \times \mathbf{F}_3 = I_p\ddot{\alpha}$$

By substituting the force components obtained from the Eqn. 3 we get the final equations of motion by considering the force and moment balance of the output link and the closed-form equations are derived in the form

$$\mathbf{M}\ddot{\mathbf{T}} + \eta = \mathbf{H}\tau$$

where

$$\mathbf{M} = \begin{bmatrix} (\sum_{i=1}^{3} \mathbf{Q}_i + m_p I_{2\times 2}) & (\sum_{i=1}^{3} \mathbf{Q}_i \mathbf{BL}_i) \\ (\sum_{i=1}^{3} \mathbf{r}_{i\perp}^T \mathbf{Q}_i) & (\sum_{i=1}^{3} \mathbf{r}_{i\perp}^T \mathbf{Q}_i \mathbf{BL}_i + I_p) \end{bmatrix}$$

$$\eta = \begin{bmatrix} \sum_{i=1}^{3} (-\mathbf{U}_i + \mathbf{Q}_i \mathbf{AL}_i \dot{\alpha}_p^2) \\ \sum_{i=1}^{3} (-\mathbf{r}_i \times \mathbf{U}_i + + \mathbf{r}_{i\perp}^T \mathbf{Q}_i \mathbf{AL}_i \dot{\alpha}_p^2) \end{bmatrix}$$

$$\mathbf{H} = \begin{bmatrix} \frac{\mathbf{d}_1}{l_1 sin(\phi_1 - \theta_1)} & \frac{\mathbf{d}_2}{l_2 sin(\phi_2 - \theta_2)} & \frac{\mathbf{d}_3}{l_3 sin(\phi_3 - \theta_3)} \\ \frac{\mathbf{r}_1 \times \mathbf{d}_1}{l_1 sin(\phi_1 - \theta_1)} & \frac{\mathbf{r}_2 \times \mathbf{d}_2}{l_2 sin(\phi_2 - \theta_2)} & \frac{\mathbf{r}_3 \times \mathbf{d}_3}{l_3 sin(\phi_3 - \theta_3)} \end{bmatrix}$$

$$\tau = \begin{bmatrix} \tau_1 & \tau_2 & \tau_3 \end{bmatrix}$$

$$\mathbf{A} = \begin{bmatrix} -cos(\alpha) & sin(\alpha) \\ -sin(\alpha) & -cos(\alpha) \end{bmatrix} \quad \mathbf{B} = \begin{bmatrix} -sin(\alpha) & -cos(\alpha) \\ cos(\alpha) & -sin(\alpha) \end{bmatrix}$$

$$\mathbf{L}_1 = \begin{bmatrix} -p/2 & -q/3 \end{bmatrix} \quad \mathbf{L}_2 = \begin{bmatrix} p/2 & -q/3 \end{bmatrix} \quad \mathbf{L}_3 = \begin{bmatrix} 0 & 2q/3 \end{bmatrix}.$$

Chapter 3

Servo Controller Design

3.1 Introduction

Given the dynamic equations of motion of the 3-DOF manipulator, the purpose of the controller is to maintain the dynamic response of the manipulator in accordance with some prespecified performance criteria. Although the control problem can be stated in such a simple manner, its solution is complicated by inertial forces, coupling reaction forces, and gravity loading (of course, the gravity effects are zero in this case, since the manipulator works in horizontal plane) on the links. This chapter aims to demonstrate the design of a proportional plus derivative (PD) controller.

3.2 The Model and Specifications

Since oscillations about the point and overshooting the point is not desired, the controller should be designed so that the system is slightly over-damped. Also the system should take less time for reaching the goal position. Therefore, the present system will be required to meet the following specifications:

1. Slightly over-damped with ζ=1.05 (chosen)
2. Settling time $t_s \leq 1sec$

The following equations are used in designing

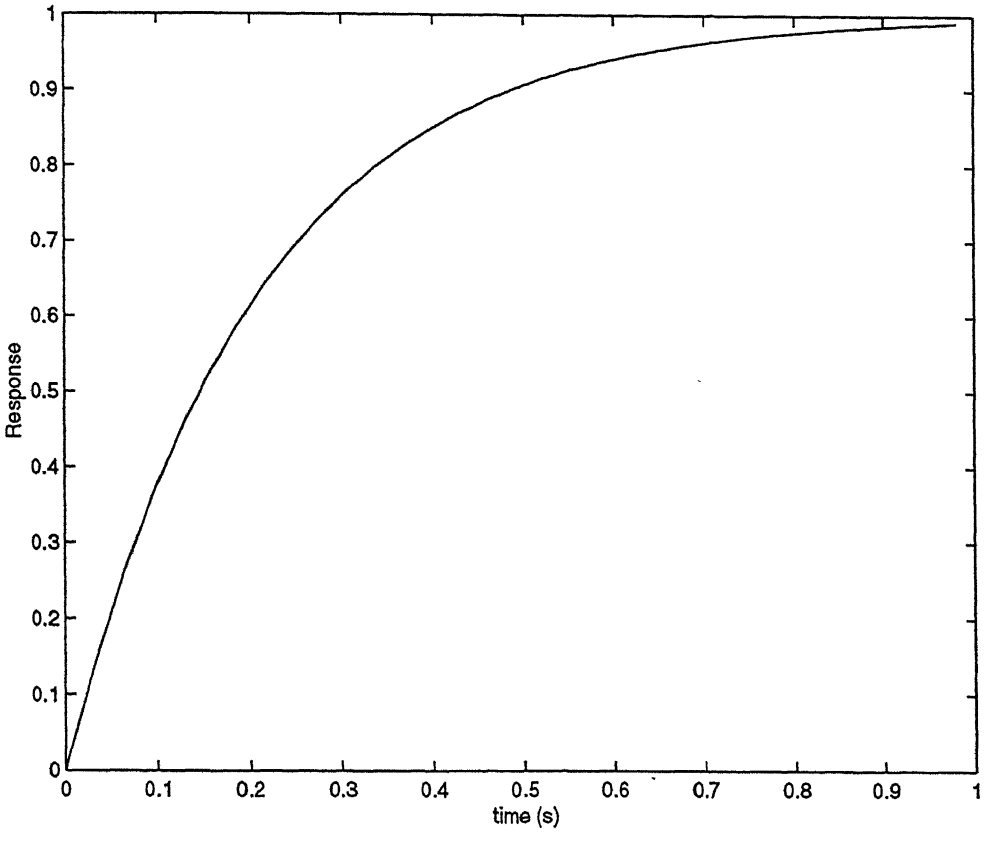

Figure 3.1: Transient Response

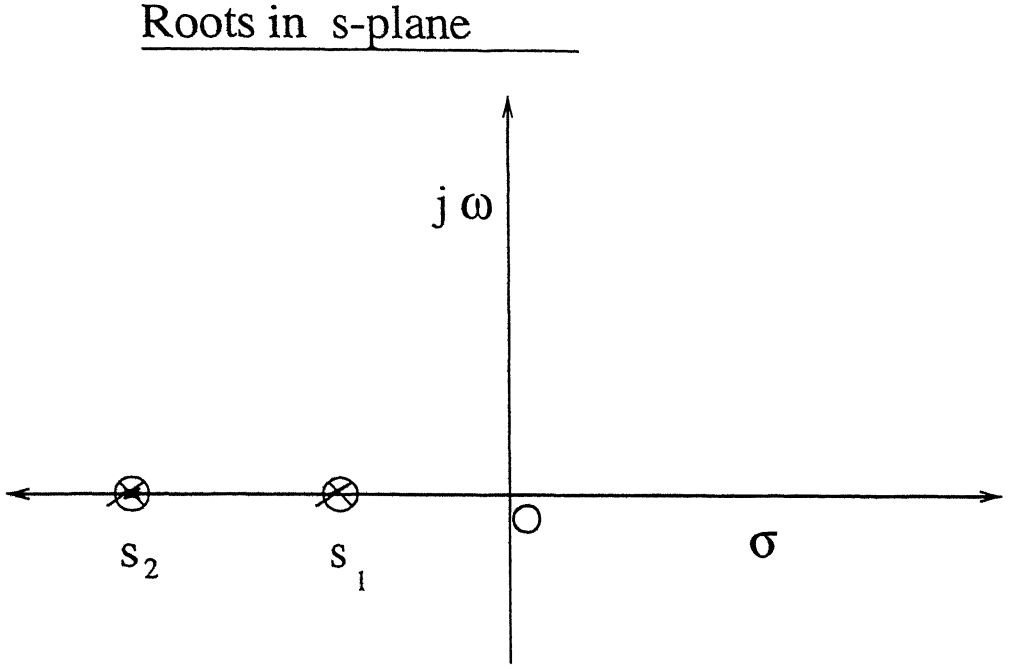

Figure 3.2: Fixing the Poles

$$c(t) = 1 + \frac{\omega_n}{2\sqrt{\zeta^2 - 1}}\left(\frac{e^{-s_1 t}}{s_1} - \frac{e^{-s_2 t}}{s_2}\right) \qquad (t \geq 0)$$

where

$$s_1 = (\zeta + \sqrt{\zeta^2 - 1})\omega_n$$

and

$$s_2 = (\zeta - \sqrt{\zeta^2 - 1})\omega_n$$

Thus, the response c(t) includes two decaying exponential terms.

So from the above Fig. 3.1, with the settling time as 1 sec, the natural frequency of the second order system is obtained as 6.5 rad/sec. With this natural frequency the poles of the system are fixed at s_1 and s_2. The poles obtained are s_2= -8.9 and s_1= -4.5 and shown in Fig. 3.2.

From the control analysis point of view, the movement of a manipulator is usually accomplished by the gross motion control in which the end-effector moves from an initial position/orientation to the vicinity of the desired target position/orientation along a

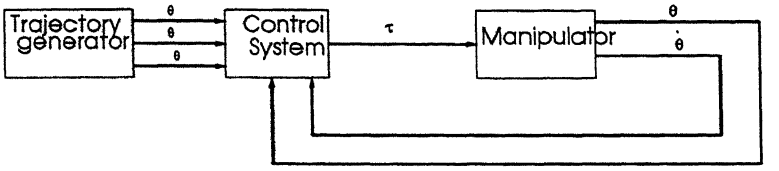

Figure 3.3: Relationship between the Trajectory Generator and the Manipulator

planned trajectory. Since we wish to cause the manipulator end-effector to follow prescribed positon trajectories, but the actuators are commanded in terms of torque, there should be some kind of control system to compute appropriate actuator commands which will realize this desired motion. Almost always these torques are computed by using feedback from the joint sensors to compute the torque required. Fig. 3.2 shows the relationship between the trajectory generator and the manipulator.

3.3 State Variable Analysis

3.3.1 Linearization

A non-linear system exhibit behavior which can be radically different for different inputs, making them difficult to control. This present section shows how to obtain the linearized model of the present non-linear model. This is accomplished by approximating the behavior of the present nonlinear system in a limited range of operation.This range of operation may be considered the operating point of the system being linearized. The final dynamic equation is

$$\mathbf{M}\ddot{\mathbf{T}} + \eta = \mathbf{H}\tau \tag{1}$$

where

H is the force-torque transformation matrix of size 3×3
η is a matrix of size 3×1 having the centripetal and coriolis components
M is the mass matrix of size 3×3

Now to find the state of the system, state variables should be taken.

State of a dynamic system is the smallest set of variables (called state variables) such that the knowledge of these variables at $t = t_0$, together with the input for $t \geq t_0$, completely determines the behavior of the system for any time $t \geq t_0$. *State variables* of a dynamic system are the smallest set of variables which determine the state of the dynamic system. All the state variables form the *State vector*. The state vector is taken as

$$\mathbf{X} = \begin{bmatrix} x \\ y \\ \alpha \\ \dot{x} \\ \dot{y} \\ \dot{\alpha} \end{bmatrix}$$

$$\dot{\mathbf{X}} = \mathbf{f}(\mathbf{X}, \tau) = \begin{bmatrix} \dot{x} \\ \dot{y} \\ \dot{\alpha} \\ \mathbf{M}^{-1}(\mathbf{H}\tau - \eta) \end{bmatrix}$$

$$\delta\dot{\mathbf{X}} = \mathbf{A}\delta\mathbf{X} + \mathbf{B}\delta\tau \tag{2}$$

where

$$\mathbf{A} = (\frac{\delta \mathbf{f}}{\delta \mathbf{X}}) \qquad \mathbf{B} = (\frac{\delta \mathbf{f}}{\delta \tau}) \tag{3}$$

$$\mathbf{A} = \begin{bmatrix} 0 & 0 & 0 & 1 & 0 & 0 \\ 0 & 0 & 0 & 0 & 1 & 0 \\ 0 & 0 & 0 & 0 & 0 & 1 \\ \mathbf{q}_1 & \mathbf{q}_2 & \mathbf{q}_3 & \mathbf{q}_4 & \mathbf{q}_5 & \mathbf{q}_6 \end{bmatrix}$$

$q_1, q_2, q_3, q_4, q_5, q_6$ are given in Appendix A.

$$B = \begin{bmatrix} 0 & 0 & 0 \\ 0 & 0 & 0 \\ 0 & 0 & 0 \\ & M^{-1}H & \end{bmatrix}$$

3.3.2 Control Design using Pole Placement

The first step before controller design is to check whether the present system is controllable. The concept of controllability involves the dependence of state variables of the system on the inputs. The system described by Eqn. 2 is controllable if it is possible to construct a control signal which, in finite time interval will transfer the system state from $\mathbf{X}(0)$ to $\mathbf{X}(t_f)$. We check this by forming the controllability matrix:

$$C = \begin{bmatrix} B & AB & ..... & A^5B \end{bmatrix}$$

The system is completely controllable if and only if the rank of the composite matrix **C** is 6 (no. of state variables).

The schematic diagram of a full-feedback system is shown in Fig. 3.3.2 where **R** is the reference input.

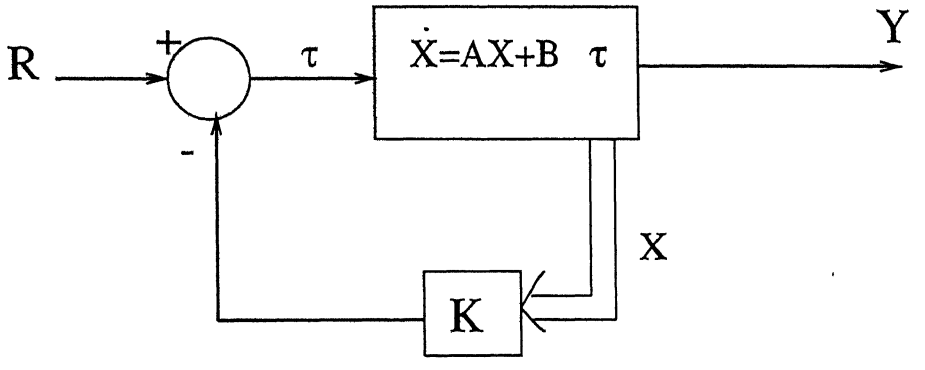

Figure 3.4: Schematic diagram of a full-feedback system

Now a technique called "pole placement" is used to obtain the desired output. Poles of a closed-loop system can be found from the characteristic equation: determinant of [sI-(A-B*K)] matrix. If desired poles can be placed into the system by designing right

control matrix (**K**), then the desired output can be obtained. So, desired poles are obtained first and then MATLAB function "place" is used to find the corresponding control matrix (**K**). The poles are placed based on upon the criteria for the controller like the settling time, damping factor, no oscillations. Then the poles are kept at

$$\lambda = \begin{bmatrix} s_{11} & s_{21} & s_{12} & s_{22} & s_{13} & s_{23} \end{bmatrix}$$

s_{1i} and s_{2i} are the two dominant poles of the i-th actuation. After fixing the poles the MATLAB function "place" is used for finding control matrix **K**. There can be many solutions for **K**, but MATLAB gives only one such solution.

$$\mathbf{K} = place(\mathbf{A}, \mathbf{B}, \lambda)$$

K is a 3×6 matrix,where position gains K_p is the first 3×3 matrix and velocity gains K_v is the second 3×3 matrix

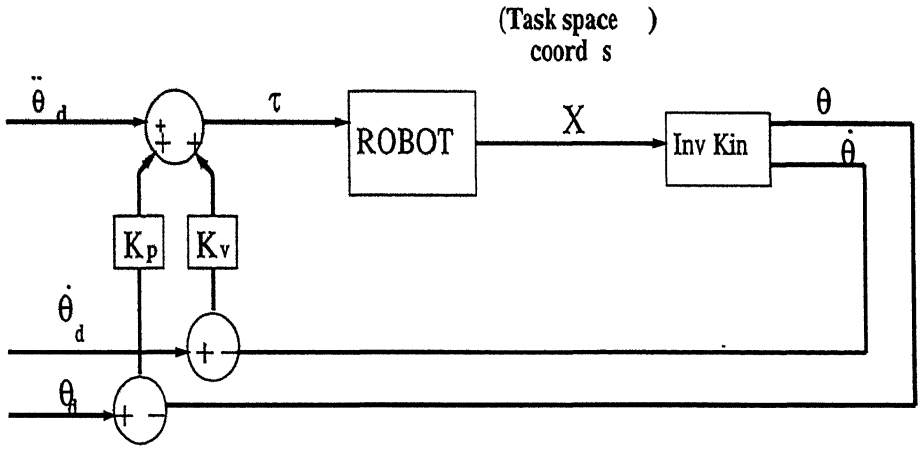

Figure 3.5: Feedback control block diagram of the 3-DOF Manipulator

The individual joint PD control is essentially a technique which attempts to control the manipulator by using local, decoupled PD's at each joint. In absence of friction or gravity, position control can be achieved by letting

$$\tau = \mathbf{K}_p\mathbf{E} + \mathbf{K}_v\dot{\mathbf{E}}$$

where $\mathbf{E}$ is the tracking error by finding the difference between the desired input value (Reference $\mathbf{R}$) and the actual output ($\mathbf{Y}$). The signal τ is now equal to the proportional gain ($\mathbf{K}_p$) times the magnitude of error plus the derivative gain ($\mathbf{K}_v$) times the derivative of the error. $\mathbf{K}_p$ and $\mathbf{K}_v$ are positive definite matrices of size 3 x 3.

The control system can then compute how much torque to send to the actuators as a function of the tracking error.

Chapter 4

Simulation Results

The dynamic formulation for the 3-DOF planar parallel manipulator has been implemented in MATLAB routines for forward dynamics (simulation). The program developed in the present work for forward dynamic simulation uses the MATLAB routine "ode45" (which is based on the 4th and 5th order Runge-Kutta formulas with adaptive step-size) for solving the system of differential equations. The program is first verified by considering the regulation problem and then verified by simulating the dynamics to track a trajectory. It is observed that the platform is successfully regulated in the desired pose and orientation within a small time interval of .35 sec.

4.1 Regulation

Example 1

The kinematic and dynamic parameters are shown in Appendix B. In Fig. 4.1, the initial conditions are assumed as

$$\mathbf{X}_0 = \begin{bmatrix} 0 & 0 & .083 & 0 & 0 & 0 \end{bmatrix}^T .$$

The desired position and orientation and their derivatives are

$$\mathbf{X}_d = \begin{bmatrix} .5 & .5 & .35 & 0 & 0 & 0 \end{bmatrix}^T$$

The position and velocity gains obtained are as follows:

$$\mathbf{K}_p = 10^3 \begin{bmatrix} .3942 & .2091 & -.9153 \\ .5112 & .2472 & -1.0435 \\ .4636 & .2339 & -1.0946 \end{bmatrix}$$

$$\mathbf{K}_v = 10^3 \begin{bmatrix} -.2983 & -.1011 & -.3053 \\ -.3656 & -.1583 & -.3503 \\ -.3847 & -.1653 & -.3651 \end{bmatrix}$$

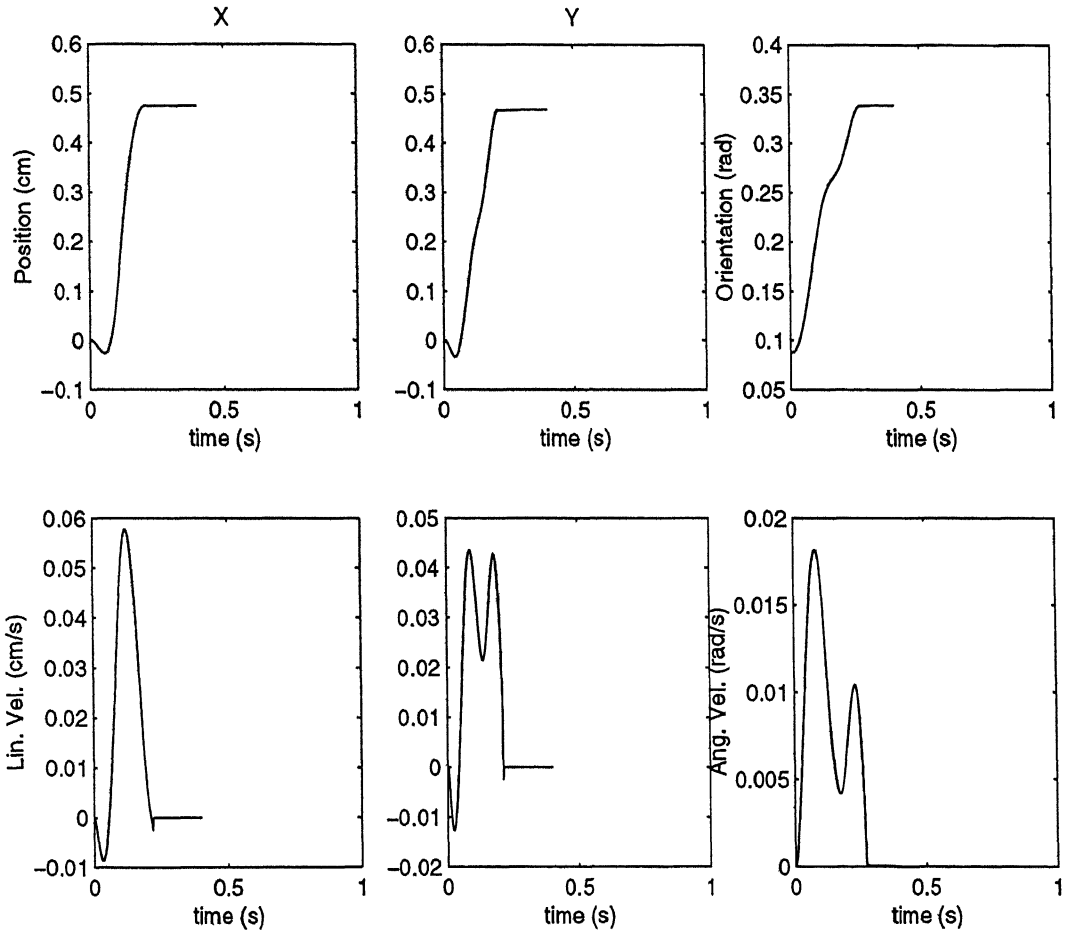

Figure 4.1: Regulation : Example 1

Example 2

In Fig. 4.2, the initial conditions are assumed as

$$\mathbf{X}_0 = \begin{bmatrix} 0 & 0 & .083 & 0 & 0 & 0 \end{bmatrix}^T.$$

The desired position and orientation and their derivatives are

$$\mathbf{X}_d = \begin{bmatrix} 0 & 0 & .35 & 0 & 0 & 0 \end{bmatrix}^T$$

The position and velocity gains obtained are as follows:

$$\mathbf{K}_p = 10^3 \begin{bmatrix} .1357 & -.0021 & -.6170 \\ .3229 & .3546 & -.7381 \\ .2815 & -.1108 & -.8736 \end{bmatrix}$$

$$\mathbf{K}_v = 10^3 \begin{bmatrix} .2320 & -.6252 & -.2016 \\ -.5629 & -.3865 & -.3604 \\ .1437 & -.054 & -.7715 \end{bmatrix}$$

Example 3

In Fig. 4.3, the initial conditions are assumed as

$$\mathbf{X}_0 = \begin{bmatrix} 0 & 0 & .083 & 0 & 0 & 0 \end{bmatrix}^T.$$

The desired position and orientation and their derivatives are

$$\mathbf{X}_d = \begin{bmatrix} -1 & -1 & .35 & 0 & 0 & 0 \end{bmatrix}^T$$

The position and velocity gains obtained are as follows:

$$\mathbf{K}_p = 10^3 \begin{bmatrix} .1732 & -.4217 & .2173 \\ .2819 & .9146 & -.1638 \\ -.7412 & .3165 & -.7693 \end{bmatrix}$$

$$\mathbf{K}_v = 10^3 \begin{bmatrix} -.6155 & -.3175 & -.2734 \\ -.5914 & -.1092 & -.699 \\ -.1317 & -.0145 & -.4763 \end{bmatrix}$$

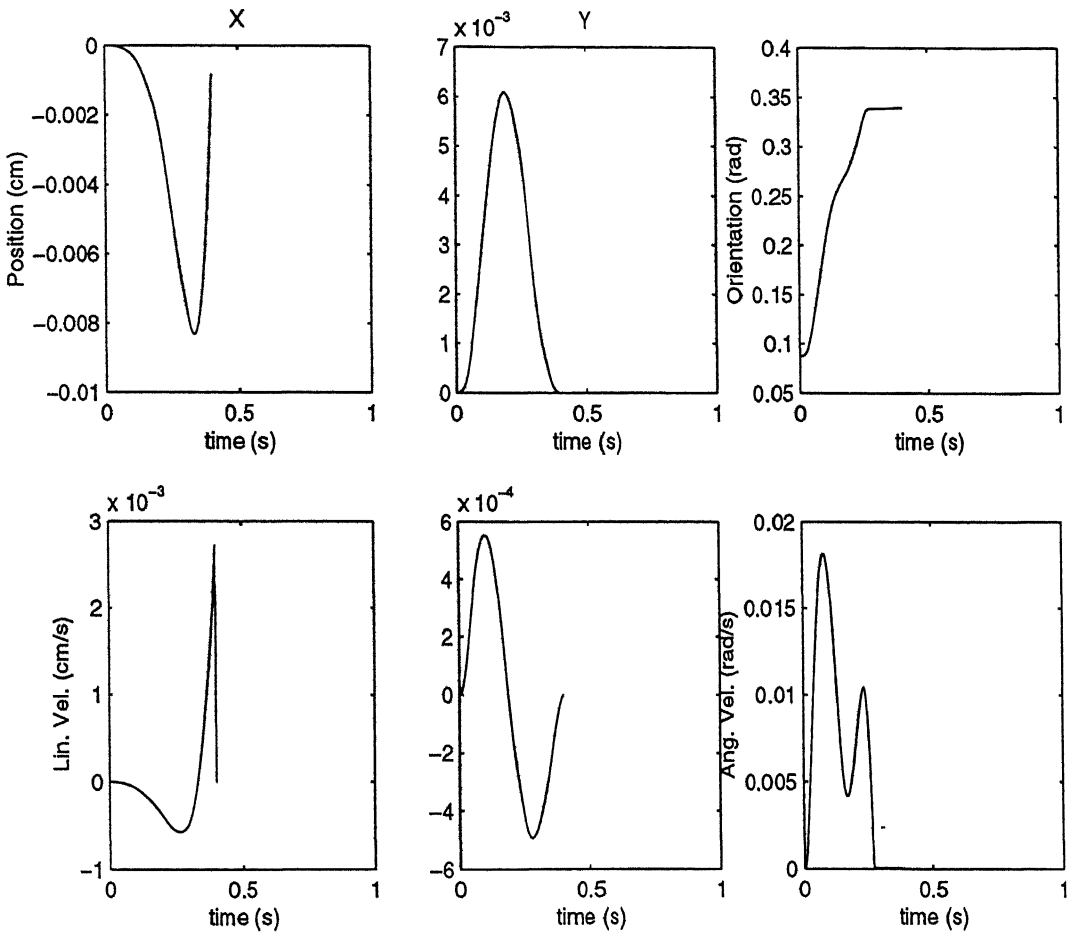

Figure 4.2: Regulation : Example 2

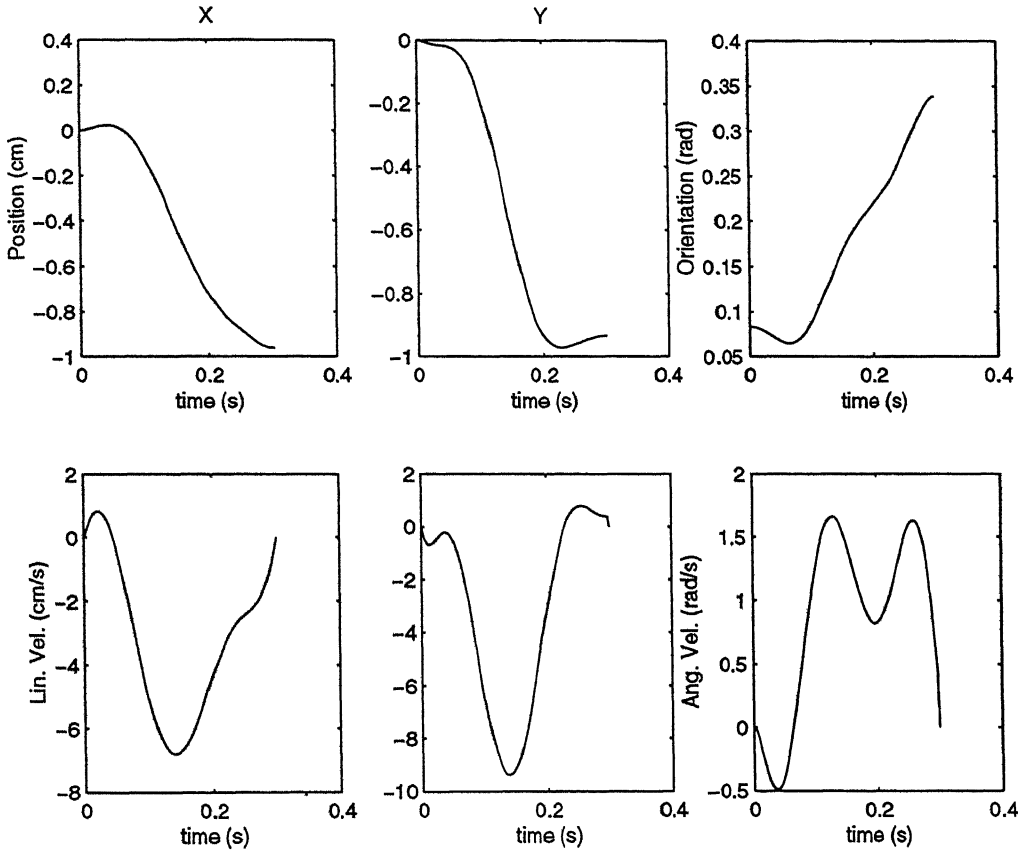

Figure 4.3: Regulation : Example 3

4.2 Tracking

Tracking is done by repeated regulation. Duration of simulation is 6.5 sec. Two examples of tracking are considered, in *example 1* end-effector traces a trajectory of

$$\mathbf{X} = \begin{bmatrix} 2sin(t) & 2cos(t) & 0 & 2cos(t) & -2sin(t) & 0 \end{bmatrix}$$

and in *example 2* along a straight line.

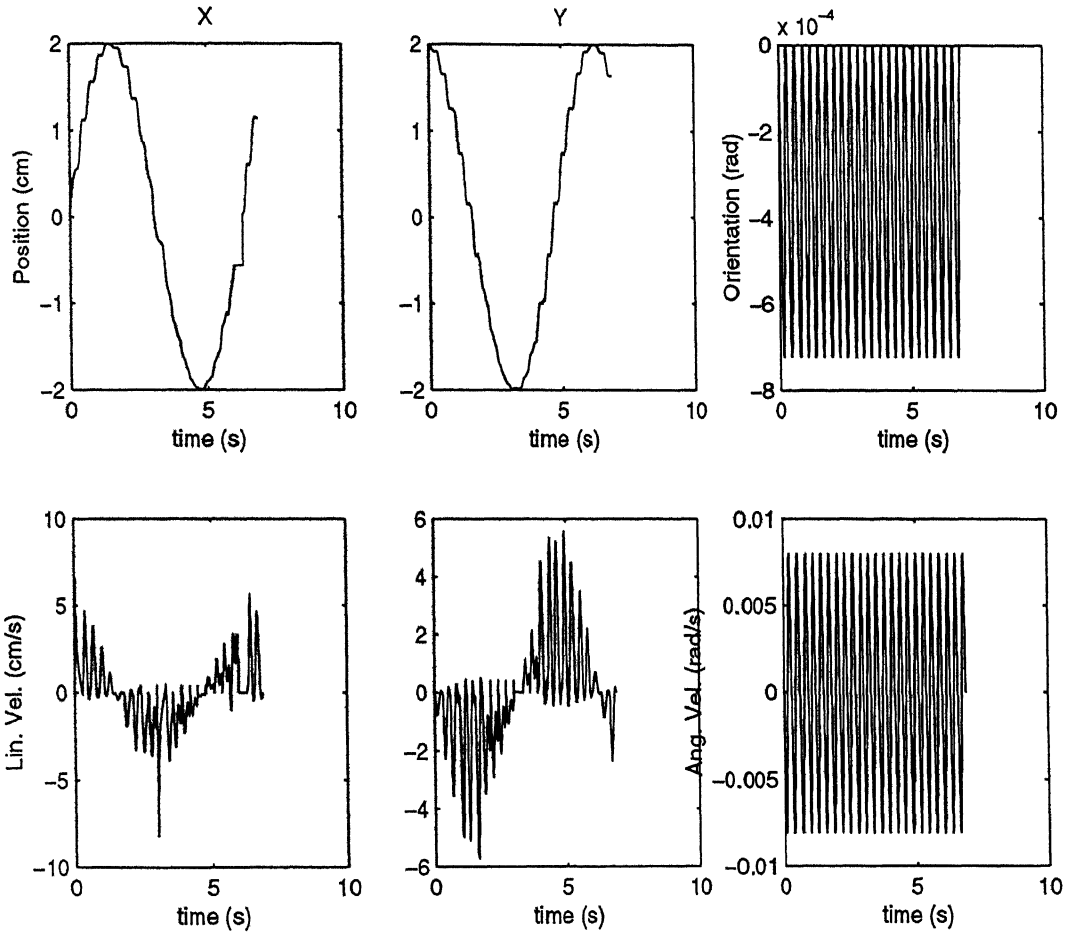

Figure 4.4: Tracking : Example 1

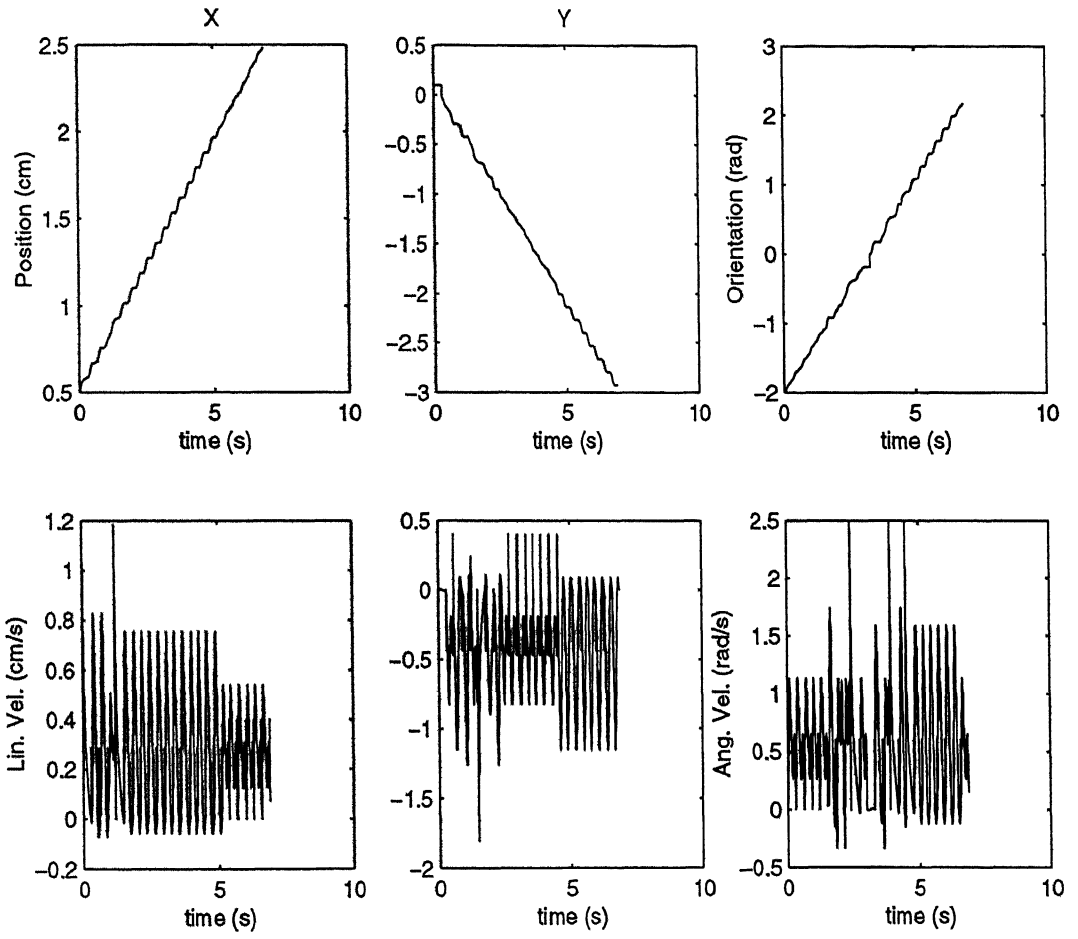

Figure 4.5: Tracking : Example 2

Chapter 5

Hardware Implementation

This chapter explains software and hardware implementation in the present work. Computers are used to program robots, and the programming is done off-line. That means the robot is not directly involved when programming takes place. By using off-line programming, the programmer has greater flexibility to carry out complex operations, and the time spent in programming is reduced. In addition the robot can remain in service while the programming takes place, thereby increasing its productivity.

5.1 Mechanical Hardware Description

The complete chain-assembly of one leg of the mechanical system is shown in Fig. 5.1.

The mechanical system mainly consists of DC motor mounted on a stand. It is jointed to the link 1 with a pin. The link 1 in turn jointed to link 2 with another pin. This chain is now pinned to the end-effector. Previously, Kalva [2] has done open-loop control of the manipulator using the stepper motors. In the present work, control is done with DC motors. So, the stepper motors are replaced with DC motors.

5.2 Control System

A personal computer based control system has been developed for the prototype parallel manipulator. The block diagram of this is shown in Fig. 5.2. The system contains three major components: a host computer, the motor driver boards, and the motors. Each board

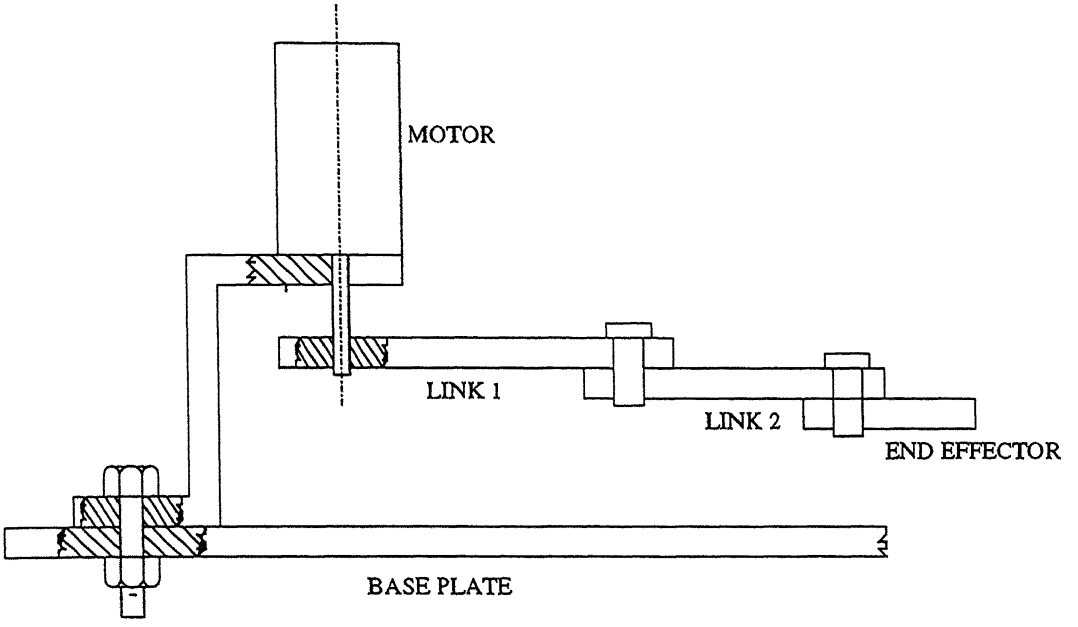

Figure 5.1: Overall Chain Assembly

controls one motor, so a total of three boards are used. The function of the DC controller is to supply the motor with appropriate torque signals, in order to implement motion in desired direction and upto desired angle. The torque is calculated based on the position and velocity errors that are obtained from the feedback of the system. The feedback from the DC motors is by the optical encoders. The error in positioning is decided by the precision of the encoder feedback. Encoder gives feedback for each .6 degrees increment of angle. So the error in positioning is within $\pm.6$. The DC motor controller includes a series of electronic switches responsible for switching the voltage of the stator coils which constitute the stator phase.

5.3 Pulse Width Modulation (PWM) for Direct Control of DC motors

DC motors can be controlled with a variable resistor or a variable resistor connected to a transistor. Even though this works well, it generates heat and hence wastage of power. The simple pulse width modulation DC motor control eliminates these problems. It controls the motor speed by driving the motor with short pulses. These pulses vary in duration

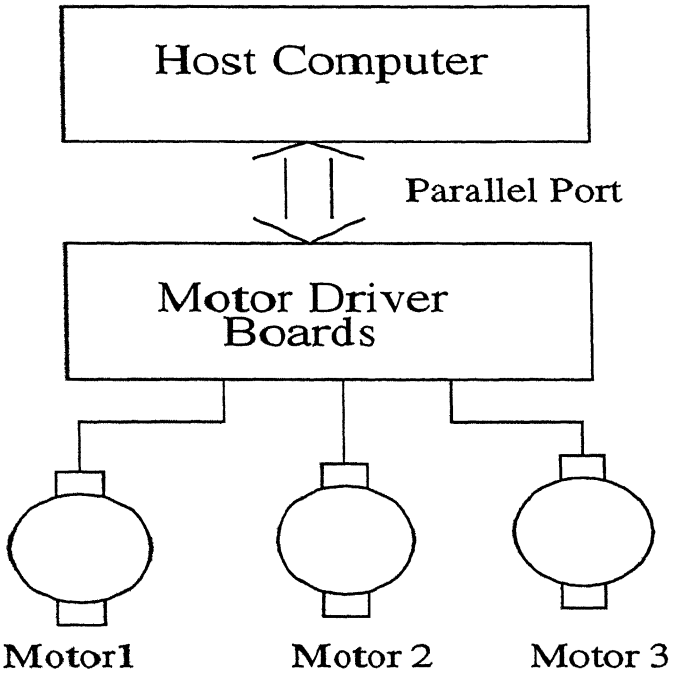

Figure 5.2: Block diagram of the control system

to change the speed of the motor. The longer the pulse width the faster the motor turns, and vice versa. The requirements of the PWM are as follows:

- The controller must provide two outputs which are modulated
- It must be possible to vary the outputs between the extremes of the first output high, the second low and the first output low and the second high. These extremes represent full speed in each direction.

5.4 Driver Circuit

The driver circuit takes signals from PC and sends signals to run the motors. It consists of three boards: card 1, card 2 and card 3. Each card drives single DC motor. Each card have 74LS244, L298 and LM324 chips. The chip 74LS244 is a 20 pin chip. It takes the control word from the parallel port and sends the signals to the motor to rotate. Depending on the control word the motor moves in forward

or reverse directions. The DC motors used are the escap motors. The encoder of the motor is connected to the LM324 and the pin connections are shown in the Fig. 5.3. The feedback can be obtained on port 379. Bits 4,5,6 gives feedback for motor 1,2,3. The motor gets its signal through L298 special 16 pin chip. The connections for the card 2 and card 3 are shown in Fig. 5.4.

5.5 Interface with PC

Interfacing links permit the manipulator to communicate with its controller and other parts of work station. Parts that do not cause the manipulator to do this task directly are called peripheral components. The microprocessor controlled manipulator can communicate with the equipment around it through connections called ports. For example, it is necessary for the manipulator to input information to the controller, and it must be able to receive information to the controller. Hence the controller is connected to the manipulator through a port. Parallel ports are the outputs of the microprocessor or computer that have flat cables connected to them with eight conductors. This parallel port is connected to the input of the controller circuit. The signals generated by the computer are fed to the controller circuit through the parallel port. For generating signals, Turbo C provide access to the I/O ports on the Pentium CPU via the predefined functions, inportb/inport and outportb/outport. For the present work, outportb and inportb are used which outputs and inputs a byte to the hardware port. This is the interface between program and DC motor control circuit. The usage of the outportb is as follows:

```
include<stdio.h>
include<dos.h>
unsigned char bits;
outportb(0x378,bits); /*output bits through 0x278 port*/
```

In the above program, 0x378 is the printer port address. Writing to this address causes data to be stored in the printers data buffer. The feedback input is taken from the port address 0x379.

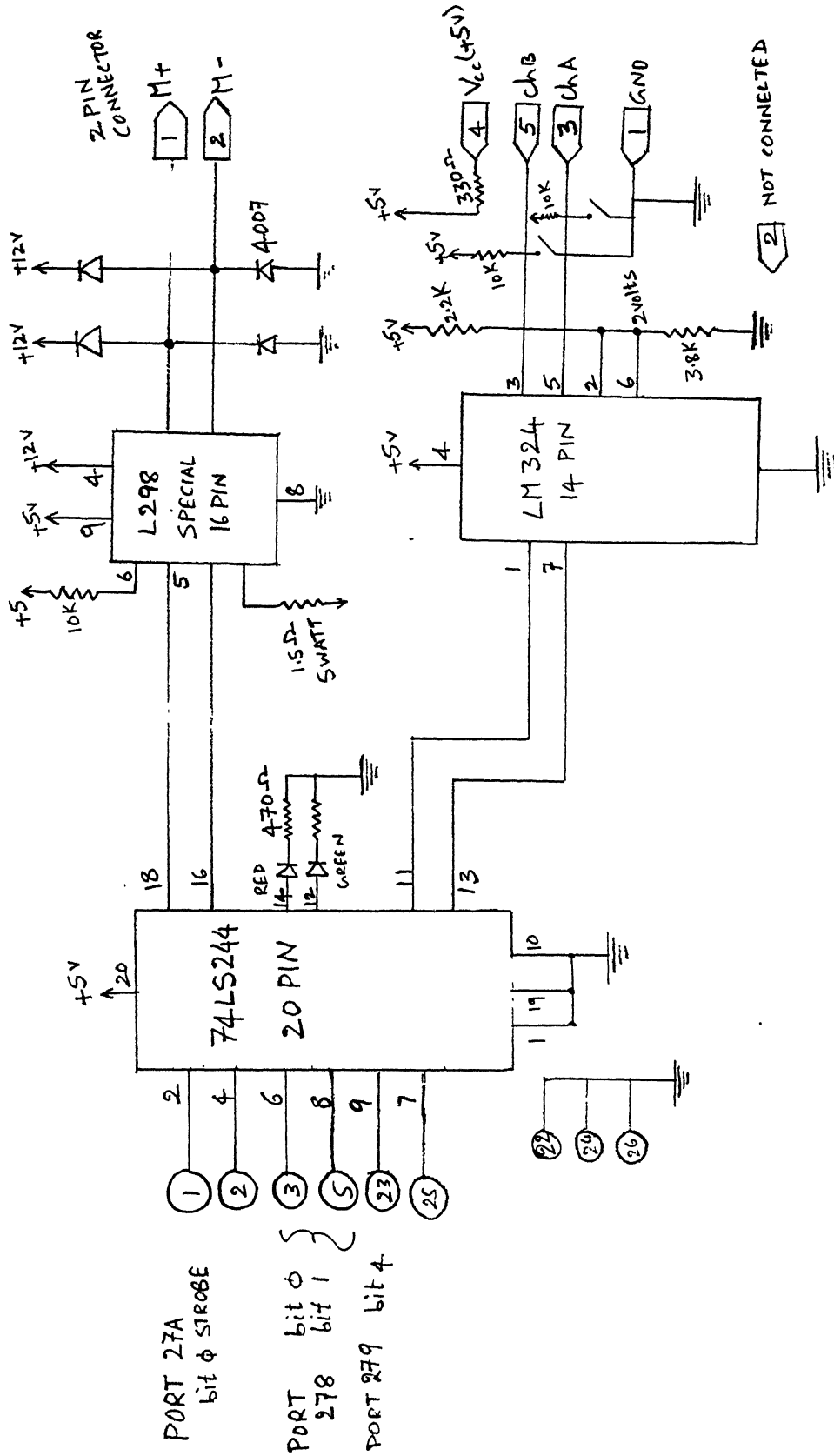

Figure 5.3: Driver circuit pin connections

Figure 5.4: Pin connections for card 2 and card 3

In the control of 3-DOF parallel manipulator three DC motors are used for activating the links. The controller circuit of each motor needs two bits, one for forward(f) and another for reverse directions(r). If both the bits are zeros or 1's then the motor will stop rotating. To control all the three motors 6 bits are required. The bit pattern for the all the three motors are shown below:

In the present work, regulation problem is dealt. This involves the positioning of

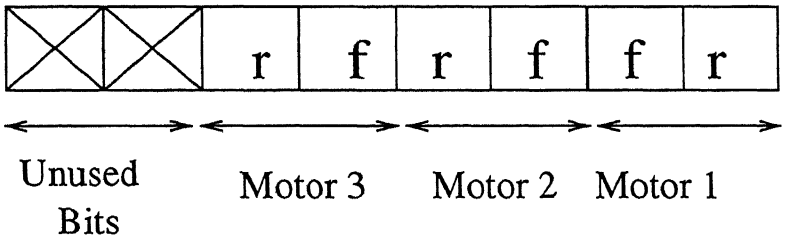

Figure 5.5: Control word bit patterns for the three motors

the end-effector at the desired point. Later with repeated regulation, the end-effector is tracked along a trajectory specified.

5.6 Software Description

The software necessary for controlling the hardware is developed in TURBO C. The software mainly consists of taking the initial position and velocity of the end-effector in joint space co-ordinates from a data file. This data file consists of initial position (joint space), orientation of the platform,velocity of the end-effector, desired position and velocity of the end-effector, position and velocity gains. The torque required is calculated based on the difference between the tracking error and error derivative. This is calculated for all the motors and accordingly each motor is activated by creating a control word. Flow chart for coordinated control of the manipulator is shown in Fig.5.6

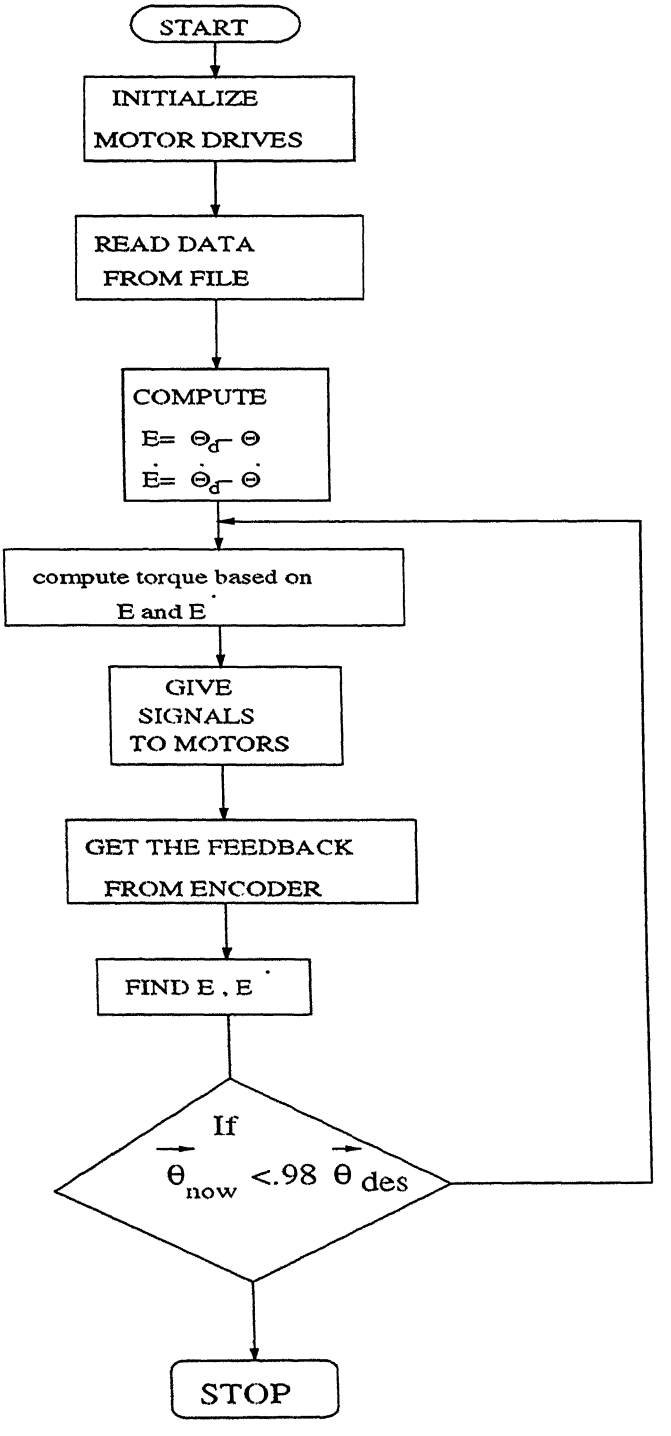

Figure 5.6: Control flow-chart

Chapter 6

Experimental Results

6.1 Testing of Performance

The main idea is to test the practical prototype to move from one postion and orientation ('x' and 'y' coordinates in *cm* and angle in degrees) to desired position and orientation. The test data is given in the Table. 6.1.

Initial Pos. and Orien.	Final Pos. and Orien.
0 0 0	0 0 40
0 0 0	2 2 15
0 0 0	-2 2 0
0 0 0	-2 -2 -10
-2 -2 0	2 2 30
2 -2 0	-2 2 0
-2 2 0	-2 -2 -15
-2 -2 0	2 -2 20

Table 6.1: Experimental Test Data

6.1.1 Accuracy

The precision with which a computed point can be attained is called the accuracy of the manipulator. The practical prototype is successfully able to move from initial configuration to the final configuration with an accuracy upto $\pm 2.0mm$ along X-axis and $\pm 3.0mm$ along Y-axis and $\pm 4^0$ orientation. Therefore, the end-effector reaches a final point which is within a radius 'R' about the desired point.

$$R = \sqrt{\Delta X_d^2 + \Delta Y_d^2} = \sqrt{2^2 + 3^2} = 3.61mm$$

Accuracy is affected by the precision of parameters appearing in the kinematic

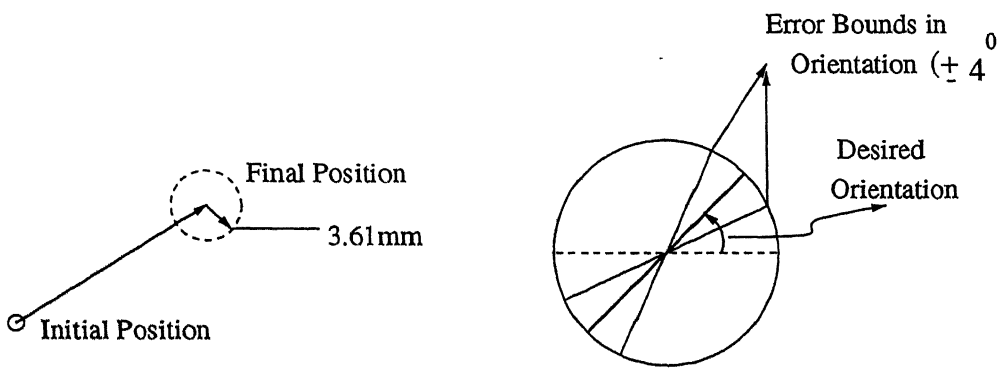

Figure 6.1: Error bounds in Positioning and Orientation

equations. Errors in Denavit-Hartenberg parameters will cause the inverse kinematic equations to calculate joint angle values which are in error. In addition, errors in estimation of dynamic parameters introduce further loss of accuracy. Calibration techniques can be devised which allow the accuracy of the manipulator to be improved through estimation of kinematic and dynamic parameters.

6.1.2 Repeatability

Repeatability is a measure of how precisely a manipulator can return to the desired configuration. The repeatability of the practical prototype is quite good. It is repeatable within an error bound of $\pm 1mm$ along X-axis and $\pm 1mm$ along Y-axis and $\pm 2^0$ in orientation.

Chapter 7

Conclusions

7.1 Summary

Closed-form dynamic equations have been derived for the 3-DOF planar parallel manipulator using Newton-Euler approach. A PD controller is designed for positioning and orienting the manipulator. Simulation results of forward dynamics are presented for both regulation and tracking problem. Experimental results for regulation are reported which are in accordance with the simulation results.

7.2 Suggestions for Future Work

- Tracking control can be done for precisely tracing the trajectory.
- More robust non-linear control laws can be applied to control the manipulator in entire workspace.
- Calibration needs to be done on this prototype manipulator to reduce the error in positioning.
- By using DC motors of higher gear reduction ratio, we can position the end-effector more precisely.

Appendix A

Intermediate Terms in the Dynamic Analysis

Detailed expressions of various terms used in the thesis.

$$\mathbf{q}_1 = -MM(1:2,1:2)\frac{\delta\boldsymbol{\eta}(1:2)}{\delta x} - MM(1:2,3)\frac{\delta\boldsymbol{\eta}(3)}{\delta x}$$

$$\mathbf{q}_2 = -MM(1:2,1:2)\frac{\delta\boldsymbol{\eta}(1:2)}{\delta y} - MM(1:2,3)\frac{\delta\boldsymbol{\eta}(3)}{\delta y}$$

$$\mathbf{q}_3 = -MM(1:2,1:2)\frac{\delta\boldsymbol{\eta}(1:2)}{\delta \alpha} - MM(1:2,3)\frac{\delta\boldsymbol{\eta}(3)}{\delta \alpha}$$

$$\mathbf{q}_4 = -MM(1:2,1:2)\frac{\delta\boldsymbol{\eta}(1:2)}{\delta \dot{x}} - MM(1:2,3)\frac{\delta\boldsymbol{\eta}(3)}{\delta \dot{x}}$$

$$\mathbf{q}_5 = -MM(1:2,1:2)\frac{\delta\boldsymbol{\eta}(1:2)}{\delta \dot{y}} - MM(1:2,3)\frac{\delta\boldsymbol{\eta}(3)}{\delta \dot{y}}$$

$$\mathbf{q}_6 = -MM(1:2,1:2)\frac{\delta\boldsymbol{\eta}(1:2)}{\delta \dot{\alpha}} - MM(1:2,3)\frac{\delta\boldsymbol{\eta}(3)}{\delta \dot{\alpha}}$$

where

$$\frac{\delta \boldsymbol{\eta}}{\delta \dot{x}} = \sum_{i=1,2,3} \begin{bmatrix} -\frac{\delta \mathbf{U_i}}{\delta \dot{x}} \\ -\mathbf{r}_i \times \frac{\delta \mathbf{U_i}}{\delta \dot{x}} \end{bmatrix}$$

$$\frac{\delta \boldsymbol{\eta}}{\delta \dot{y}} = \sum_{i=1,2,3} \begin{bmatrix} -\frac{\delta \mathbf{U_i}}{\delta \dot{y}} \\ -\mathbf{r}_i \times \frac{\delta \mathbf{U_i}}{\delta \dot{y}} \end{bmatrix}$$

$$\frac{\delta \boldsymbol{\eta}}{\delta \dot{\alpha}} = \sum_{i=1,2,3} \begin{bmatrix} -\frac{\delta \mathbf{U_i}}{\delta \dot{\alpha}} \\ -\mathbf{r}_i \times \frac{\delta \mathbf{U_i}}{\delta \dot{\alpha}} \end{bmatrix}$$

$$\mathbf{A} = \begin{bmatrix} -cos(\alpha) & sin(\alpha) \\ -sin(\alpha) & -cos(\alpha) \end{bmatrix} \quad \mathbf{B} = \frac{d\mathbf{A}}{d\alpha} \quad \mathbf{C} = -\mathbf{A} \;\; MM = inv(\mathrm{M});$$

$$\mathbf{k} = \mathbf{QAL}_1 + \mathbf{QAL}_2 + \mathbf{QAL}_3$$

$$\mathbf{U}_i = \mathbf{AV}_{ui} + \mathbf{BV}_{di} + \mathbf{CV}_{0i}$$

$$\frac{\delta \boldsymbol{\eta}}{\delta x} = \frac{\delta \mathbf{k}}{\delta x}\dot{\alpha}^2 - \sum_{i=1,2,3} \frac{\delta \mathbf{U}_i}{\delta x}$$

$$\frac{\delta \boldsymbol{\eta}}{\delta y} = \frac{\delta \mathbf{k}}{\delta y}\dot{\alpha}^2 - \sum_{i=1,2,3} \frac{\delta \mathbf{U}_i}{\delta y}$$

$$\frac{\delta \boldsymbol{\eta}}{\delta \alpha} = \frac{\delta \mathbf{k}}{\delta \alpha}\dot{\alpha}^2 - \sum_{i=1,2,3} \frac{\delta \mathbf{U}_i}{\delta \alpha}$$

where,

$$\frac{\delta \mathbf{U}_i}{\delta x} = \mathbf{A}\frac{\delta \mathbf{V}_{ui}}{\delta x} + \mathbf{B}\frac{\delta \mathbf{V}_{di}}{\delta x}$$

$$\frac{\delta \mathbf{U}_i}{\delta y} = \mathbf{A}\frac{\delta \mathbf{V}_{ui}}{\delta y} + \mathbf{B}\frac{\delta \mathbf{V}_{di}}{\delta y}$$

$$\frac{\delta \mathbf{U}_i}{\delta \dot{x}} = \mathbf{A}\frac{\delta \mathbf{V}_{ui}}{\delta \dot{x}} + \mathbf{B}\frac{\delta \mathbf{V}_{di}}{\delta \dot{x}} + \mathbf{C}\frac{\delta \mathbf{V}_{0i}}{\delta \dot{x}}$$

$$\frac{\delta \mathbf{U}_i}{\delta \dot{y}} = \mathbf{A}\frac{\delta \mathbf{V}_{ui}}{\delta \dot{y}} + \mathbf{B}\frac{\delta \mathbf{V}_{di}}{\delta \dot{y}} + \mathbf{C}\frac{\delta \mathbf{V}_{0i}}{\delta \dot{y}}$$

$$\frac{\delta \mathbf{U}_i}{\delta \alpha} = \frac{\delta \mathbf{A}}{\delta \alpha}\mathbf{V}_u i + \frac{\delta \mathbf{B}}{\delta \alpha}\mathbf{V}_d i + \frac{\delta \mathbf{C}}{\delta \alpha}\mathbf{V}_0 i$$

$$\frac{\delta \mathbf{k}}{\delta x} = \frac{\delta \mathbf{k}}{\delta y} = \frac{\delta \mathbf{U}_i}{\delta \dot{\alpha}} = 0$$

$$\frac{\delta \mathbf{k}}{\delta \alpha} = \sum_{i=1,2,3} \mathbf{Q}\frac{\delta \mathbf{A}}{\delta \alpha}\mathbf{L}_i$$

$$\frac{\delta \mathbf{V}_0}{\delta \dot{x}} = \frac{2(\dot{x}cos(\phi) + \dot{y}sin(\phi))cos(\phi)}{sin(\phi-\theta)^2}\mathbf{c} + \frac{2(\dot{x}cos(\theta) + \dot{y}sin(\theta))cos(\theta)}{sin(\phi-\theta)^2}\mathbf{d}$$

$$\frac{\delta \mathbf{V}_0}{\delta \dot{y}} = \frac{2(\dot{x}cos(\phi) + \dot{y}sin(\phi))sin(\phi)}{sin(\phi-\theta)^2}\mathbf{c} + \frac{2(\dot{x}cos(\theta) + \dot{y}sin(\theta))sin(\theta)}{sin(\phi-\theta)^2}\mathbf{d}$$

$$\frac{\delta \mathbf{V}_d}{\delta x} = -\mathbf{B}\frac{\mathbf{r}_{d\perp}\mathbf{c}^T\mathbf{V}_0}{lsin^2(\phi-\theta)}cos(\phi-\theta)$$

$$\frac{\delta \mathbf{V}_d}{\delta y} = -\mathbf{B}\frac{\mathbf{r}_{d\perp}\mathbf{c}^T\mathbf{V}_0}{lcos^2(\phi-\theta)}sin(\phi-\theta)$$

$$\frac{\delta \mathbf{V}_d}{\delta \dot{x}} = \frac{\mathbf{r}_{d\perp}\mathbf{d}^T}{lsin(\phi-\theta)}\frac{\delta \mathbf{V}_0}{\delta \dot{x}} - \frac{2\mathbf{r}_d(\dot{x}cos(\phi)+\dot{y}sin(\phi))cos(\phi)}{l^2sin(\phi-\theta)^2}$$

$$\frac{\delta \mathbf{V}_d}{\delta \dot{y}} = \frac{\mathbf{r}_{d\perp}\mathbf{d}^T}{lsin(\phi-\theta)}\frac{\delta \mathbf{V}_0}{\delta \dot{y}} - \frac{2\mathbf{r}_d(\dot{x}cos(\phi)+\dot{y}sin(\phi))sin(\phi)}{l^2sin(\phi-\theta)^2}$$

$$\frac{\delta \mathbf{V}_u}{\delta x} = \frac{\mathbf{c}_\perp\mathbf{d}^T\mathbf{V}_0}{sin^2(\phi-\theta)}cos(\phi-\theta) + \frac{\mathbf{r}_{u\perp}\mathbf{c}^T\mathbf{V}_0}{usin^2(\phi-\theta)}cos(\phi-\theta)$$

$$\frac{\delta \mathbf{V}_u}{\delta y} = \frac{\mathbf{c}_\perp\mathbf{d}^T\mathbf{V}_0}{cos^2(\phi-\theta)}sin(\phi-\theta) + \frac{\mathbf{r}_{u\perp}\mathbf{c}^T\mathbf{V}_0}{ucos^2(\phi-\theta)}sin(\phi-\theta)$$

$$\frac{\delta \mathbf{V}_u}{\delta \dot{x}} = (\frac{\mathbf{c}_\perp d^T}{sin(\phi-\theta)} - \frac{\mathbf{r}_{u\perp}\mathbf{c}^T}{usin(\phi-\theta)})\frac{\delta \mathbf{V}_0}{\delta \dot{x}} + \frac{2(\dot{x}cos(\phi)+\dot{y}sin(\phi))cos(\phi)}{lsin(\phi-\theta)^2}\mathbf{c}$$

$$-\mathbf{r}_u\frac{2(\dot{x}cos(\theta)+\dot{y}sin(\theta))cos(\theta)}{u^2sin(\phi-\theta)^2}$$

$$\frac{\delta \mathbf{V}_u}{\delta \dot{y}} = (\frac{\mathbf{c}_\perp d^T}{sin(\phi-\theta)} - \frac{\mathbf{r}_{u\perp}\mathbf{c}^T}{usin(\phi-\theta)})\frac{\delta \mathbf{V}_0}{\delta \dot{y}} + \frac{2(\dot{x}cos(\phi)+\dot{y}sin(\phi))sin(\phi)}{lsin(\phi-\theta)^2}\mathbf{c}$$

$$-\mathbf{r}_u\frac{2(\dot{x}cos(\theta)+\dot{y}sin(\theta))sin(\theta)}{u^2sin(\phi-\theta)^2}$$

Appendix B

Kinematic and Dynamic Parameters and Motor Specifications

B.1 Kinematic and Dynamic parameters

Base coordinates = $\begin{bmatrix} -11.3 & 11.2 & -1.6 \\ -12 & -9.9 & 11 \end{bmatrix}$

Link lenghts:

Length of the upper link 'u': 9.5 cm

Length of the lower link 'l': 12.75 cm

Length of each side of the platform 'p': 5 cm

Mass of the links:

Mass of the upper link 'm_u': .03 kg

Mass of the lower link 'm_d': .025 kg

Mass of the platform 'm_p': .03 kg

Moment of inertias of the links:

Moment of inertia of the upper link 'I_u': 1.6256 $kgcm^2$

Moment of Inertia of the lower link 'I_d': 0.752 $kgcm^2$

Moment of Inertia of the platform 'I_p': 2.3 $kgcm^2$

B.2 Motor Specifications

Stall Torque 720 $kgmm^2$
Max. speed 9000 rpm
Rotor Moment of Inertia .0714 $kgcm^2$

Bibliography

[1] Prasun Choudhury and Bhaskar Dasgupta. A general strategy based on the newton-euler approach for the dynamic formulation of parallel manipulators. *Mechanism and Machine Theory*, (34):801–824, 1998.

[2] Kalva Santosh. Design and development of a 3-dof planar parallel manipulator. Master's thesis, Dept of Mechanical Engg, 1999.

[3] Marvin Minsky. Manipulator design vignettes. *MIT AIL Memo 267*, oct 1972.

[4] K.H.Hunt. Structural kinematics of in-parallel-actuated robot-arms. *Trans. of ASME J of Mechanical Design*, (105):705–712, 1993.

[5] J.Angeles O.Ma. Direct kinematics and dynamics of a planar three-dof parallel manipulator. *Trans. ASME,J of Mechanical Design*, 32(2), 1993.

[6] Raymond G.Jacquot. An optimal control approach to robot manipulator pole placement. *IEEE Journal of Robotics and Automation*, 3(2):65–69, 1988.